Checkpoint protein expression in the tumor microenvironment defines the outcome of classical Hodgkin lymphoma patients

Kristiina Karihtala, Suvi-Katri Leivonen, Marja-Liisa Karjalainen-Lindsberg, Fong Chun Chan, Christian Steidl, Teijo Pellinen and Sirpa Leppä

Supplementary Material

Supplementary Methods

Patients and samples

All patients in this study were diagnosed between years 1993-2012 and treated or followed at the Helsinki University Hospital according to national guidelines. Disease staging, treatment and determination of the Epstein-Barr virus (EBV) status have been described previously [1]. Clinical data were collected retrospectively from medical records, and FFPE tumor samples from pathological archives. Seventy-nine patients overlapped between the two cohorts (Supplementary Figure S1). Patient data were handled according to Good Scientific Practice (GSP) Guidelines.

In silico immunophenotyping

CIBERSORT algorithm uses a set of reference gene expression values (an LM22 signature matrix of 547 genes), which are considered to represent specific cell types. Based on those values, the algorithm infers the cell type proportions from the gene expression dataset using support vector regression. CIBERSORT also derives a p-value for the deconvolution for each sample using Monte Carlo sampling, providing a measure of confidence in the results. To run CIBERSORT, normalized gene expression data were uploaded to the CIBERSORT web portal (http://cibersort.stanford.edu/) and the algorithm run using the default LM22 signature matrix at 1000 permutations.

Immunohistochemistry

Based on the haematopathologist's evaluation, the most representative tumor areas from the FFPE tumor tissue samples were selected for the TMA construction. The TMAs included one to six replicate cores from the same tumor tissue.

The tissue microarray (TMA) core was defined positive for the Hodgkin Reed-Sternberg (HRS) cell status for HLA-ABC, β_2 microglobulin (B2M) and HLA-DR, if over 50% of the HRS cells were membrane-positive for the marker in the core. The cases where the HRS cell status was discordant between replicate cores from same patient were excluded from further analysis. HRS cells with membranous staining (negative vs. positive) of HLA-ABC were evaluable in 109 (83%), B2M in 110 (84%) and HLA-DR in 107 (82%) patients from the whole IHC cohort.

Multiplex immunohistochemistry

The primary and secondary antibodies used in seven mIHC panels are shown in Supplementary Table 1. mIHC for panels 1 to 5 was performed using protocol described earlier [1, 2]. Methods for the panels 6 and 7 differed from the rest by inclusion of an additional second staining round as well as different imaging scanner. In the panels 6 and 7, after the first-round staining and whole-slide imaging of the TMAs, the coverslips were removed by soaking the slides in wash buffer at 4°C. Then the previous Alexa Fluor staining was bleached by soaking the slides in TBS buffer containing 25 mM NaOH and 4,5% H2O2. The antibodies from the first-round staining were denatured by heating the slides in 1 mM Tris/10mM EDTA pH 9 solution for 20 minutes at 99°C. The second-round staining was performed with the antibodies and secondary labels as shown in Supplementary Table 1. For panels 1 to 5, fluorescence images were acquired using Metafer 5 scanning and imaging platform (MetaSystems, Germany) consisting of AxioImager.Z2 (Zeiss, Germany) microscope (see more detailed specifications for the instrumentation in REF). Panels 6 and 7 imaging was done using Zeiss Axio Scan.Z1 with Zeiss 20X (0.8NA, M27) Plan-Apochromat objective, Hamamatsu ORCA-Flash 4.0 V2 Digital CMOS camera (16-bit; 0.325 μm/pixel resolution), and Zeiss Colibri.7 LED Light Source. The filter specifications were: DAPI cube (Zeiss Filter Set 02), FITC cube (Zeiss Filter Set 38 HE), Cy3 cube (Chroma Technology Corp 49004 ET

CY3/R), Cy5 cube (Chroma Technology Corp 49006 ET CY5), Cy7 cube (Chroma Technology Corp 49007 ET CY7).

If a single antibody or identical combination of two antibodies were applicable more than in one panel, the mean values from the cell proportions between these panels were used in the analysis. Correlations for cell proportions between separate panels correlated well with each other: $CD3^+$ (r_s=0.586-0.847, *P*<0.001), $CD3^+CD4^+$ (r_s= 0.404-0.757, *P*<0.001), $CD3^+CD8^+$ (r_s= 0.735-0.933, *P*<0.001), IDO-1^+ (r_s=0.939, *P*<0.001), PD-1^+ (r_s=0.550, *P*<0.001), TIM-3^+ (r_s=0.897, *P*<0.001), LAG-3^+ (r_s=0.908, *P*<0.001), $CD68^+$ (r_s=0.581-0.792, *P*<0.001), $CD163^+$ (r_s=0.960-0.978, *P*<0.001), $CD30^+$ (r_s=0.381-0.525, *P*<0.001), IDO-1^+CD3^+ (r_s=914, *P*<0.001), IDO-$1^+CD3^+/CD3^+$ (r_s=0.921, *P*<0.001), IDO-1^+CD3^+/IDO-1^+ (r_s=0.613, *P*<0.001).

Statistical Methods

Freedom from treatment failure (FFTF) was defined as the time between diagnosis and lymphoma progression or relapse, and in the lack of these, to the last date of contact information. Overall survival (OS) was defined as the time between diagnosis and death due any cause. A level of probability below 0.05 was considered significant. All comparisons were two tailed.

References

1. Karihtala K, Leivonen SK, Bruck O, et al. Prognostic Impact of Tumor-Associated Macrophages on Survival Is Checkpoint Dependent in Classical Hodgkin Lymphoma. *Cancers (Basel)*. 2020;12(4):877.
2. Blom S, Paavolainen L, Bychkov D, et al. Systems pathology by multiplexed immunohistochemistry and whole-slide digital image analysis. *Sci Rep*. 2017;7(1):15580.

Supplementary Tables

Supplementary Table S1. Multiple immunohistochemistry panel design.

	Secondary antibody for detection	Panel 1	Panel 2	Panel 3	Panel 4	Panel 5	Panel 6	Panel 7
1st round	**TSA-488**	M-anti-FOXP3 (Abcam; 20034) 1:400	M-anti-CD8 (Dako; M7103) 1:1000	M-anti-CD30 (Cell Marque; 130M-94) 1:100	R-anti-CD163 (Abcam; 188571) 1:5000	M-anti-Anti-PD-1 (LS Bio; B12784) 1:100	M-anti-CD3 (Abcam; 17143) 1:200	M-anti-PD-1 (LSBio; 12784) 1:200
	TSA-555	R-anti-CD3 (Thermo; EP449e) 1:1500	R-anti-CD3 (Thermo; EP449e) 1:1500	R-anti-PD-L1 (CST; 13684) 1:200	R-anti-CD4 (Abcam; 133616) 1:1000	R-Anti-CD4 (Abcam; 133616) 1:1000	R-anti-Lag-3 (Abcam; 180187) 1:400	R-anti-Lag-3 (Abcam; 180187) 1:400
	Alexa-647	M-anti-CD8 (Dako; M7103) 1:300	M-anti-CD68 (Abcam; 955) 1:100	M-anti-CD68 (Abcam; 955) 1:100	R-anti-IDO1 (CST; 86630) 1:400	M-Anti-CD8 (Dako; M7103) 1:300	R-anti-Tim-3 (CST; 45208) 1:100	R-anti-Tim-3 (CST; 45208) 1:100
	Alexa-750	R-anti-CD4 (Abcam; 133616) 1:25	R-anti-IDO1 (CST; 86630) 1:200	R-anti-CD163 (Abcam; 188571) 1:200	M-anti-CD3* (Abcam; 17143) 1:2000	R-Anti-CD3 (Thermo; EP449e) 1:100	M-anti-CD8 (Dako; M7103) 1:200	M-anti-CD68 (Abcam; 955) 1:50
2nd round	**TSA-Alexa 647**						M-anti-CD30 (Dako; M0751) 1:100	M-anti-CD30 (Dako; M0751) 1:100
	Alexa-750						R-anti-CD4 (Abcam; 133616) 1:50	R-anti-CD163 (Abcam; 188571) 1:200

CST indicates Cell Signaling Technologies; M, mouse; R, rabbit; TSA, tyramide signal amplification.
*CD3 signal was amplified using TSA-biotin-streptavidin-750 detection

Supplementary Table S2. Cox regression analysis at univariate level showing association of clinical characteristics with FFTF and OS in the IHC cohort.

Clinical characteristic	FFTF HR	95% CI	*P*	OS HR	95% CI	*P*
Higher age (≥45 years)	1.71	0.77-3.79	0.184	**7.73**	**1.92-31.07**	**0.004**
High Stage (IIB-IV)	**8.02**	**2.43-26.50**	**0.001**	6.50	0.81-52.02	0.078
Female gender	0.64	0.31-1.34	0.235	0.61	0.16-2.28	0.464
Other histological cHL subtype than NS	1.28	0.54-3.04	0.579	2.41	0.59-9.84	0.221
EBV status (positive)	0.81	0.33-2.02	0.653	**4.10**	**1.10-15.38**	**0.036**

Boldface font indicates statistical significance (*P*<0.05).
CI indicates confidence interval; EBV, Ebstein-Barr virus; FFTF, freedom from treatment failure; HR, hazard ratio; NS, nodular sclerosis; OS, overall survival.

Supplementary Table S3. Results of pathway analysis with the 90-gene T cell signature.

Pathway	***P***	**Genes**
The Co-Stimulatory Signal During T cell Activation	2.18E-04	*ITK, CD3D, CD80, CD3E, ICOS, CD247, LCK, CTLA4, CD28*
T cell receptor signaling pathway	9.50E-04	*ITK, CD3D, CD3E, CD247, PIK3CD, CTLA4, CARD11, CD40LG, FYN, ICOS, LCK, ZAP70, IKBKB, NFATC2, CD28*
Stathmin and breast cancer resistance to antimicrotubule agents	0.005399	*CDK1, CD3D, CD3E, CD247, CD2*
Lck and Fyn tyrosine kinases in initiation of TCR Activation	0.008752	*CD3D, FYN, CD3E, CD247, LCK, ZAP70*
NF-kappa B signaling pathway	0.011851	*TRAF2, CCL19, NFKB2, ATM, CARD11, CD40LG, CCL21, BCL2, LCK, ZAP70, IKBKB, TNFAIP3, LTB, LTA, TRAF3*
Activation of Csk by cAMP-dependent Protein Kinase Inhibits Signaling through the T Cell Receptor	0.047393	*CD3D, CD3E, CD247, LCK, ZAP70*
T Cytotoxic Cell Surface Molecules	0.088683	*CD3D, CD3E, CD247, CD2, CD28*
T Helper Cell Surface Molecules	0.088683	*CD3D, CD3E, CD247, CD2, CD28*
NO2-dependent IL 12 Pathway in NK cells	0.093413	*IL12RB2, STAT4, CD3D, CD3E, CD247, CD2*
Primary immunodeficiency	0.098667	*CD3D, CD3E, CD40LG, ICOS, LCK, ZAP70, IL2RG*

Supplementary Table S4. Distribution of baseline characteristics between subgroups of patients with T cell-inflamed and non-T cell-inflamed TME in the gene expression cohort.

Gene expression cohort	Non-T cell-inflamed TME	T cell-inflamed TME	*P*
Number of patients	21	67	
Gender			
Male	11 (52)	31 (48)	0.712
Female	10 (48)	36 (52)	
Age			
<45 years	10 (48)	45 (67)	0.106
≥45 years	11 (52)	22 (33)	
Stage (n=87)			
I-IIA	12 (57)	20 (30)	**0.026**
IIB-IV	9 (43)	46 (70)	
Histological subtype			
Nodular sclerosis	16 (76)	49 (73)	0.781
Other	5 (24)	18 (27)	
EBV status (n=72)			
Negative	9 (60)	37 (65)	0.725
Positive	6 (40)	20 (35)	

Boldface font indicates statistical significance ($P<0.05$).

Supplementary Table S5. List of DEGs (cut off: absolute fold change ≥2, adjusted *P*<0.05) between patients with T cell-inflamed and non-T cell-inflamed TME. Genes with positive fold change (FC) are expressed more in T cell-inflamed TME and with negative FC in non-T cell-inflamed TME.

Gene	Log2FC	adj.P.Val	Gene	Log2FC	adj.P.Val	Gene	logFC	adj.P.Val
LTB	1.619892	6.63E-15	*CD5*	1.258079	1.32E-08	*MRC1*	-1.69346	3.54E-05
CD3D	1.285091	2.99E-13	*CLEC7A*	-1.24298	1.67E-08	*CXCL3*	-1.09282	4.46E-05
CD6	1.190702	3.25E-13	*SERPING1*	-1.41089	5.30E-08	*CCL18*	-2.09063	4.70E-05
TCF7	1.599657	3.50E-13	*FCGR2B*	-1.48719	8.51E-08	*CD22*	1.328799	4.91E-05
MSR1	-2.25411	1.25E-12	*TREM1*	-1.75282	1.00E-07	*MARCO*	-1.40552	6.15E-05
CD28	1.275722	1.25E-12	*CD3G*	1.089511	1.26E-07	*IL21*	1.27033	6.42E-05
CXCR5	1.464924	1.89E-12	*SPP1*	-2.14745	2.54E-07	*CCL19*	1.165687	6.76E-05
CCR7	1.400563	3.31E-12	*CCL8*	-1.62114	4.05E-07	*FN1*	-2.15532	6.82E-05
CD3E	1.201935	4.30E-12	*CD14*	-1.2378	4.98E-07	*MS4A1*	1.300345	6.82E-05
ITK	1.137903	8.22E-12	*IL22RA2*	1.803831	4.98E-07	*IL8*	-1.74531	0.000166
C3AR1	-1.38252	1.06E-11	*PDGFRB*	-1.23088	8.31E-07	*KLRB1*	1.396259	0.000177
IL21R	1.022331	1.45E-11	*CR2*	1.674908	1.05E-06	*CD19*	1.090851	0.000179
AXL	-1.42297	4.65E-11	*CD36*	-1.40976	1.33E-06	*CD79A*	1.160483	0.000298
CD163	-2.44524	4.65E-11	*ITGA5*	-1.07563	2.14E-06	*CCR4*	1.022567	0.00031
CD7	1.396715	5.88E-11	*SIGLEC1*	-1.54998	2.25E-06	*CCL11*	-1.71085	0.000407
CD40LG	1.240036	8.79E-11	*SH2D1A*	1.210462	2.78E-06	*ANXA1*	-1.14377	0.00045
CDH1	1.379615	1.45E-10	*CCL21*	2.051941	3.20E-06	*CCL23*	-1.46401	0.000497
SELL	1.335917	1.96E-10	*PPARG*	-1.096	4.78E-06	*S100A8*	-1.26028	0.000837
CD276	-1.34717	4.37E-10	*TNFRSF18*	1.030738	5.92E-06	*CCL13*	-2.13943	0.000841
SLC11A1	-1.63959	4.67E-10	*IFI27*	-1.12093	6.64E-06	*CLEC5A*	-1.01434	0.000948
CEBPB	-1.28523	4.67E-10	*PLAU*	-1.17413	9.32E-06	*CXCL13*	1.368432	0.001148
FCGR2A	-1.56494	5.08E-10	*NRP1*	-1.05578	9.58E-06	*F13A1*	-1.51994	0.001245
ITGAM	-1.25975	5.33E-10	*CTSL*	-1.02365	1.16E-05	*IL1RN*	-1.12975	0.001288
CCR1	-1.16149	1.01E-09	*CFD*	-1.35124	1.16E-05	*COL3A1*	-1.89505	0.001478
LRP1	-1.82598	1.06E-09	*COLEC12*	-1.05151	1.40E-05	*C1QB*	-1.24002	0.001681
GZMM	1.103937	2.05E-09	*CD209*	-1.7569	2.08E-05	*C1QA*	-1.06928	0.002468
ICOS	1.310375	2.23E-09	*IL1R1*	-1.07312	2.33E-05	*C1R*	-1.08151	0.008454
FCGR3A	-1.95941	2.30E-09	*TNFRSF13C*	1.092682	2.33E-05	*PRAME*	1.200592	0.009291
ZAP70	1.058599	3.67E-09	*CD79B*	1.138641	2.62E-05	*CXCL12*	-1.09554	0.013658
MME	-2.29396	8.71E-09	*TREM2*	-1.28986	2.82E-05	*CCL26*	-1.17342	0.039535

Supplementary Table S6. Distribution of the baseline characteristics between the four immune cell clusters.

Characteristic	TAMs low T cells low	TAMs low. $CD4^+$ T cells high	TAMs and CTLs high	TAMs high. T cells low	*P*
Number of patients	45	25	31	30	
Gender					
Male	20 (44)	11 (44)	15 (48)	14 (47)	0.984
Female	25 (56)	14 (56)	16 (52)	16 (53)	
Age (years)					
<45	38 (84)	23 (92)	22 (71)	17 (57)	**0.008**
≥45	7 (16)	2 (8)	9 (29)	13 (43)	
Histological subtype					
Nodular sclerosis	34 (76)	23 (92)	20 (64.5)	25 (83)	0.080
Other	11 (24)	2 (8)	11 (35.5)	5 (17)	
Stage (n=130)					
I-IIA	23 (52)	12 (48)	10 (32)	11 (37)	0.290
IIB-IV	21 (48)	13 (52)	21 (68)	19 (63)	
EBV status (n=123)					
Negative	32 (71)	20 (80)	18 (64)	19 (76)	0.606
Positive	13 (29)	5 (20)	10 (36)	6 (24)	
T cell-inflamed TME (n=79)					
Yes	23 (96)	14 (100)	16 (70)	6 (33)	**<0.001**
No	1 (4)	0 (0)	7 (30)	12 (67)	

Boldface font indicates statistical significance ($P<0.05$).

Supplementary Table S7. Distribution of baseline characteristics between patients with high and low checkpoint molecule expression in the TME.

Characteristic	High	Low	*P*
Number of patients	41	84	
Gender			
Male	22 (54)	34 (40.5)	0.164
Female	19 (46)	50 (59.5)	
Age (years)			
<45	30 (73)	68 (81)	0.321
≥45	11 (27)	16 (19)	
Histological subtype			
Nodular sclerosis	27 (66)	71 (84.5)	**0.017**
Other	14 (34)	13 (15.5)	
Stage (n=124)			
I-IIA	14 (34)	39 (47)	0.174
IIB-IV	27 (66)	44 (53)	
EBV status (n=120)			
Negative	25 (64)	61 (75)	0.202
Positive	14 (36)	20 (25)	
T cell-inflamed TME (n=74)			
Yes	17 (65)	39 (81)	0.129
No	9 (35)	9 (19)	
HLA-ABC (n=108)			
Negative	23 (66)	52 (71)	0.560
Positive	12 (34)	21 (29)	
B2M (n=108)			
Negative	22 (65)	64 (86.5)	**0.009**
Positive	12 (35)	10 (13.5)	
HLA-DR (n=105)			
Negative	23 (66)	42 (60)	0.570
Positive	12 (34)	28 (40)	

Boldface font indicates statistical significance ($P<0.05$).

Supplementary Table S8. Cox regression analysis using categorical variables at univariate level showing association of high checkpoint molecule expression with OS after stratification with histological subtype and B2M status.

OS risk factor	HR (95% CI)	*P*
High checkpoint expression	5.19 (1.29-20.88)	**0.020**
Stratified with histological subtype (nodular sclerosis vs other)	4.78 (1.16-19.68)	**0.030**
Stratified with B2M status (neg vs pos)	4.79 (1.08-21.27)	**0.039**

Supplementary Table S9. List of DEGs (cut off: absolute fold change ≥ 2, adjusted *P*<0.05) between patients with high and low checkpoint expression in the IHC cohort. Genes with negative fold change are upregulated in patients with high checkpoint expression.

Gene	logFC	adjusted *P*-value
IFNG	-1.38905	5.40E-07
LAG3	-1.78946	5.40E-07
C1QB	-1.88237	2.80E-06
CXCL10	-2.06529	2.80E-06
C1QA	-1.62944	5.57E-06
C2	-1.20476	5.60E-06
SLAMF7	-1.30358	7.03E-06
CXCL9	-2.68856	7.58E-06
LILRB2	-1.23228	1.67E-05
CD8B	-1.05373	2.47E-05
CCL17	3.015582	3.95E-05
TLR8	-1.04897	3.95E-05
GZMK	-1.14486	4.02E-05
CD8A	-1.18923	6.05E-05
CXCL11	-1.66996	6.43E-05
GZMH	-1.03495	9.20E-05
STAT1	-1.00698	0.000116
IDO1	-1.27855	0.000153
CCR4	1.077071	0.000186
CCL22	1.951421	0.000314
FCGR1A	-1.06242	0.000314
FCGR3A	-1.31185	0.000794
FCER1G	-1.23025	0.001538
HSD11B1	-1.02811	0.003664
IL27	-1.0975	0.004103
SIGLEC1	-1.01623	0.006751
FCER2	1.014965	0.008287
IL22RA2	1.114341	0.008293
S100A8	-1.06239	0.009468
TPSAB1	1.14709	0.014062
CD163	-1.11416	0.017898
PRAME	1.111963	0.030722
CHIT1	-1.42133	0.039689
IL9	1.434833	0.044021

Supplementary Figure Legends

Supplementary Figure S1. Study design. Study material consists of clinical data and formalin-fixed paraffin-embedded diagnostic tumor tissue samples from two cohorts of patients with primary classical Hodgkin lymphoma.

Supplementary Figure S2. Unsupervised hierarchical clustering of the gene expression data. NanoString nCounter digital gene expression profiling with PanCancer Immune Profiling Panel was used to assess the expression of 770 immune response genes from 88 cHL samples of the gene expression cohort. After exclusion of housekeeping genes and the genes expressed in less than 10% of the samples, the final analysis included 706 genes. Log_2 transformed, z-score normalized data were clustered using Euclidean distance with ward.D linkage. The six main gene clusters were named based on the genes enriched in the clusters, as determined by pathway analysis.

Supplementary Figure S3. Correlations between gene expression and protein marker levels. Correlations by Spearman rank analysis between the proportions of distinct T cell markers, macrophage markers and checkpoint molecules with the corresponding gene expression levels. The cell proportions according to mIHC analysis are depicted on the x-axis and corresponding gene expression (log_2 values) according to Nanostring analysis on the y-axis.

Supplementary Figure S4. Correlations between CIBERSORT and mIHC analysis. Correlations of T cell and TAM proportions by Spearman rank analysis between CIBERSORT and mIHC analysis. The cell proportions according to mICH analysis are depicted on the x-axis and corresponding cell proportions according to CIBERSORT on the y-axis.

Supplementary Figure S5. Associations of different T cell phenotypes with HRS cells' membranous HLA-complexes. Associations of proportions of different T cell phenotypes in the

TME with **A)** HLA-ABC **B)** B2M **C)** HLA-DR (negative vs positive) membrane expressions in HRS cells. P-values were calculated using Mann-Whitney test.

Supplementary Figure S6. Expression of checkpoint molecules in T cells and TAMs. Median proportions of checkpoint molecule-expressing T cells ($CD3^+$) and TAMs ($CD68^+$) from all corresponding checkpoint molecule expressing cells determined by mIHC analysis. P-values were calculated using Mann-Whitney test.

Supplementary Figure S7. Checkpoint expression according to the T cell and TAM phenotypes. Proportions of distinct checkpoint expressing immune cells **A)** from all $CD4^+$ T cells ($CD3^+CD4^+$) and CTLs ($CD3^+CD8^+$) and **B)** from all $CD68^+$ and $CD163^+$ TAMs as determined by mIHC analysis. P-values were calculated using Mann-Whitney test.

Supplementary Figures

Supplementary Figure S1. Study design.

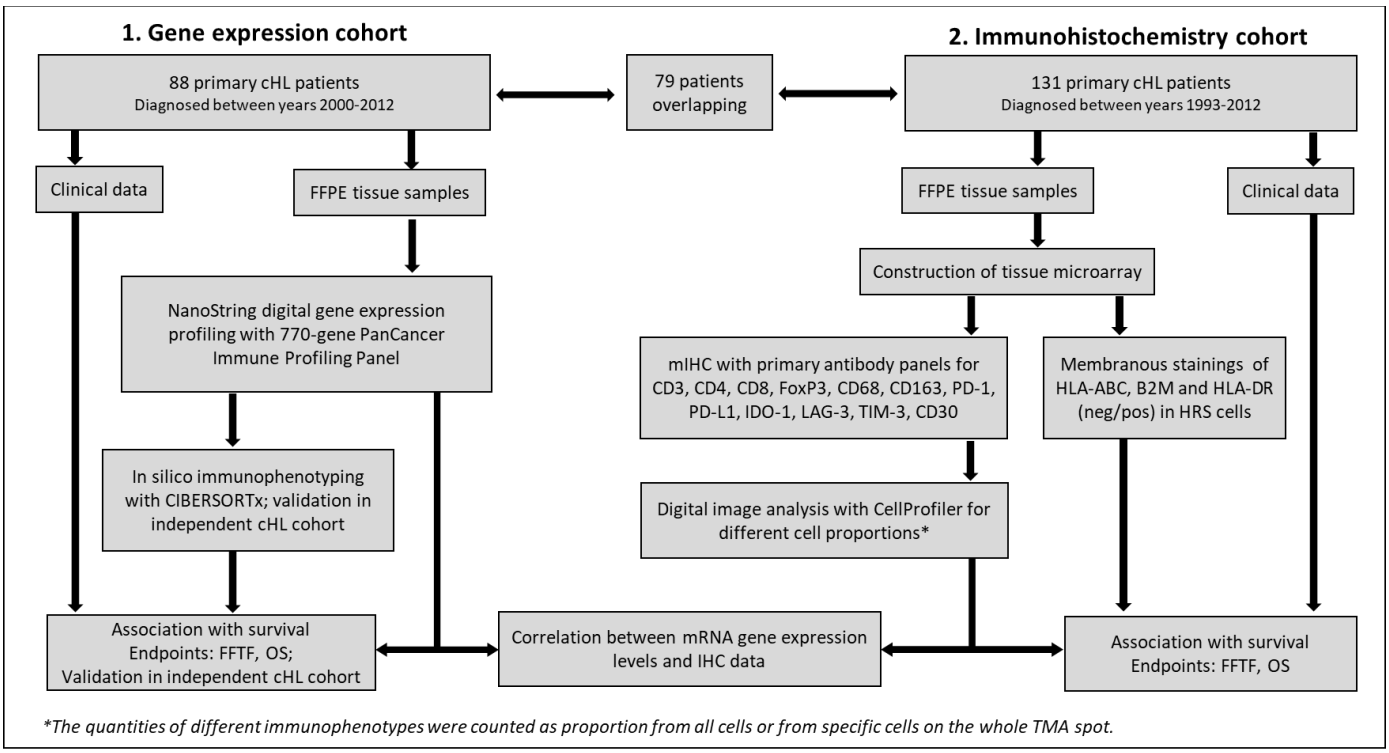

FFPE, formalin-fixed paraffin-embedded; PD-1, programmed cell death protein 1; PD-L1, programmed cell death-ligand 1; IDO-1, indoleamine 2,3-dioxygenase 1; LAG-3, lymphocyte-activation gene 3; TIM-3, T-cell immunoglobulin and mucin domain containing protein 3; B2M, β^2 microglobulin; mIHC, multiplex immunohistochemistry; FFTF, freedom from treatment failure; OS, overall survival.

Supplementary Figure S2. Unsupervised hierarchical clustering of the gene expression data.

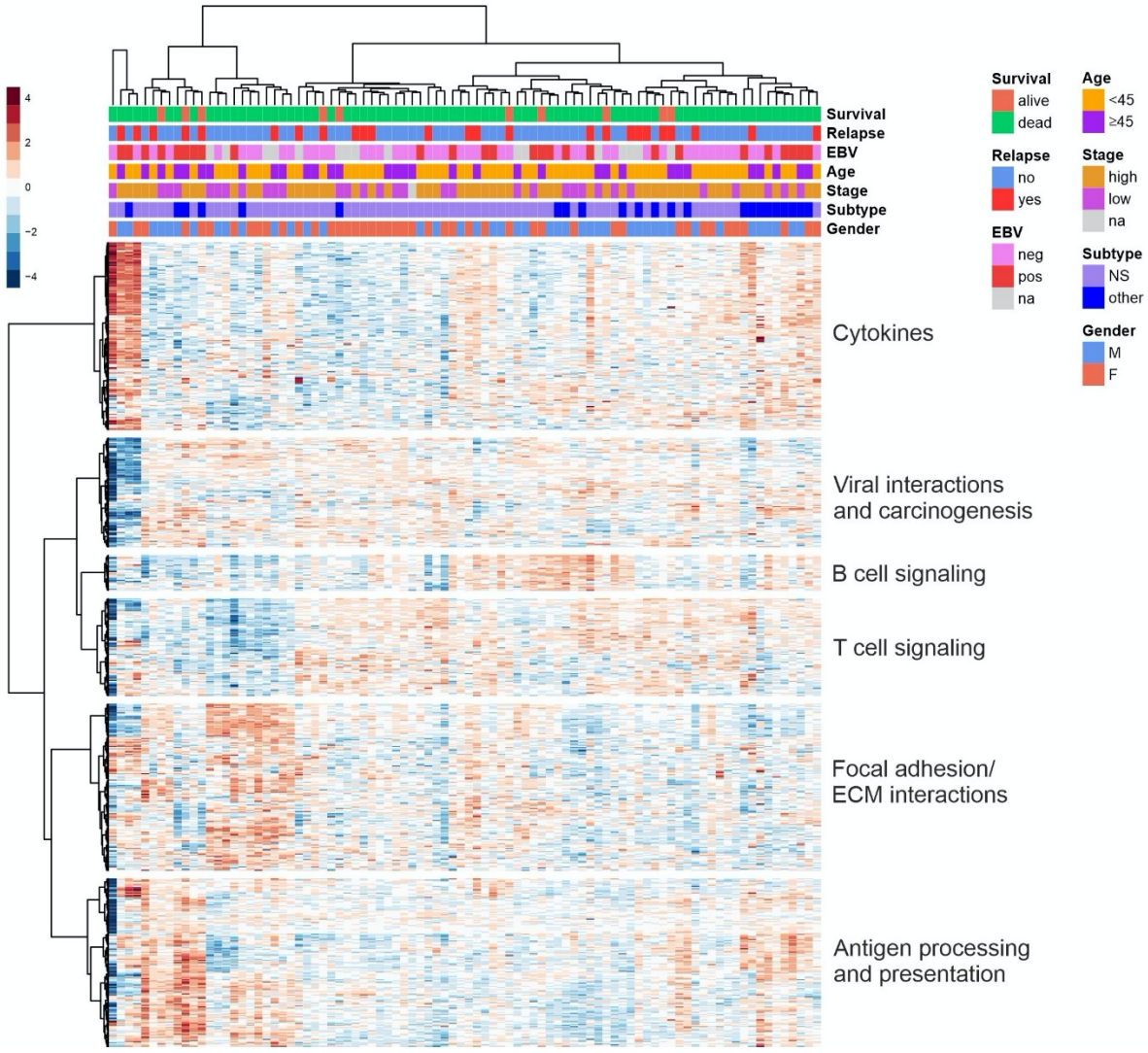

Supplementary Figure S3. Correlations between gene expression and protein marker levels.

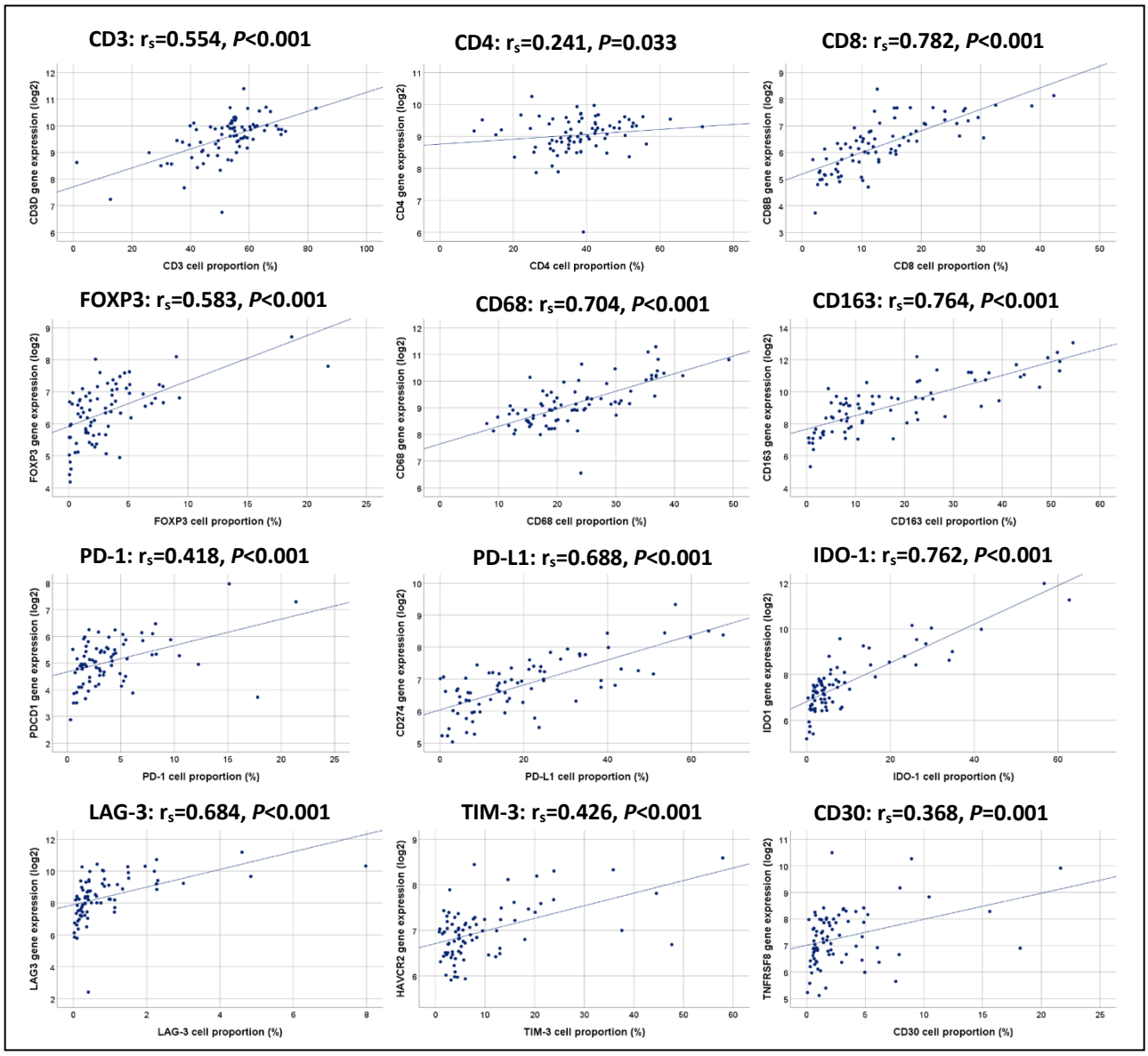

Supplementary Figure S4. Correlations between CIBERSORT and mIHC analysis.

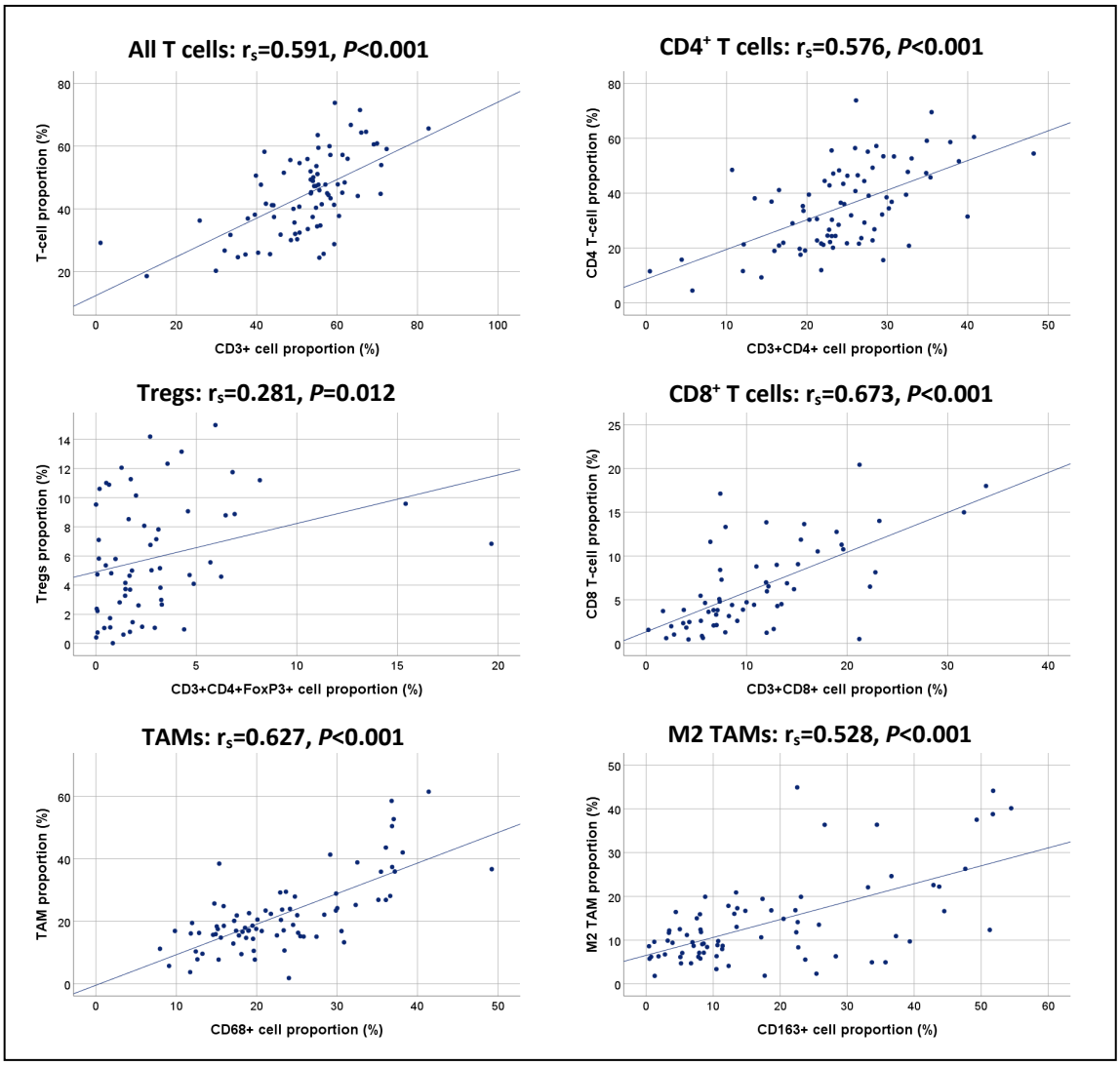

Supplementary Figure S5. Associations of different T cell phenotypes with HRS cells' membranous HLA-complexes.

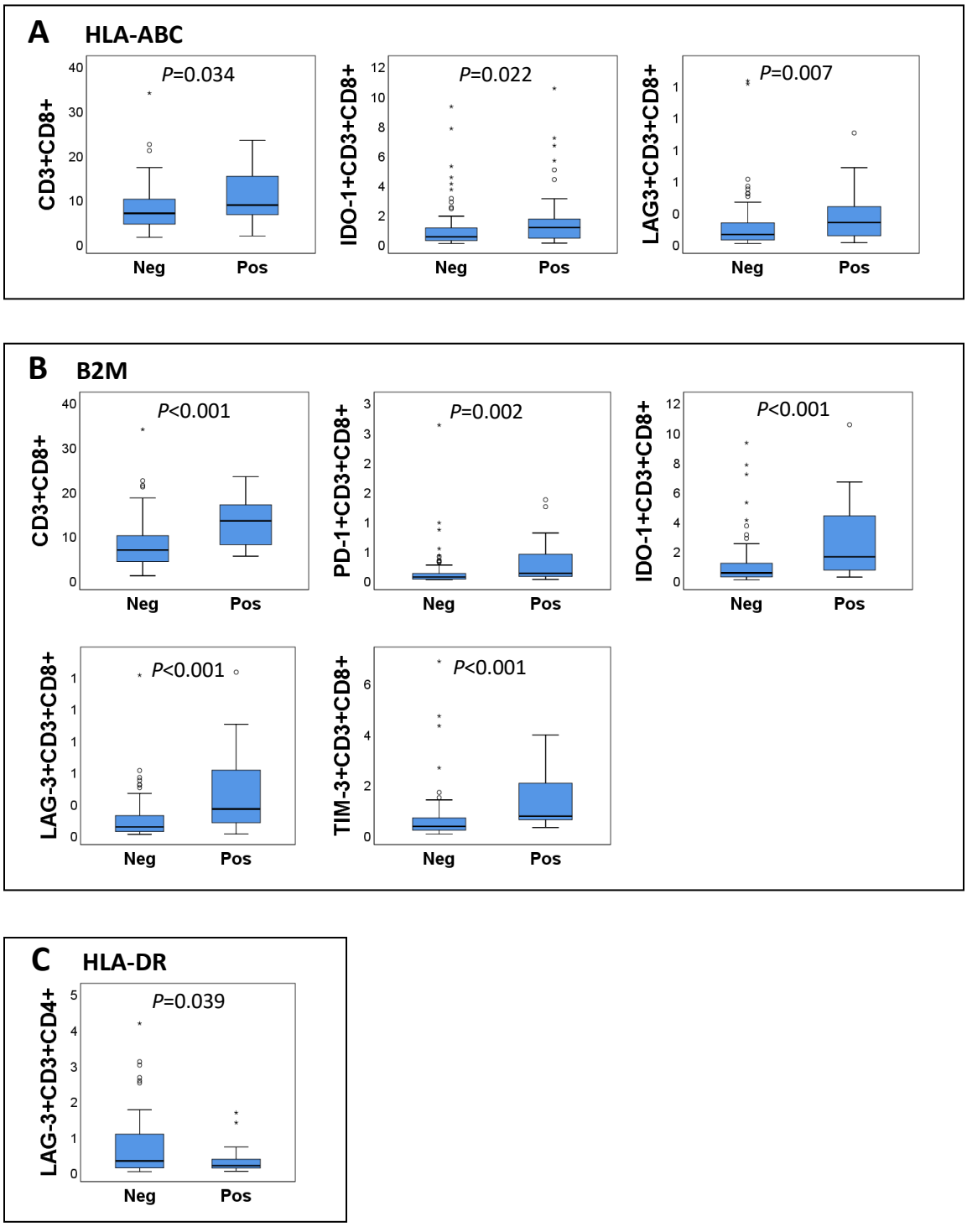

Supplementary Figure S6. Expression of checkpoint molecules in T cells and TAMs.

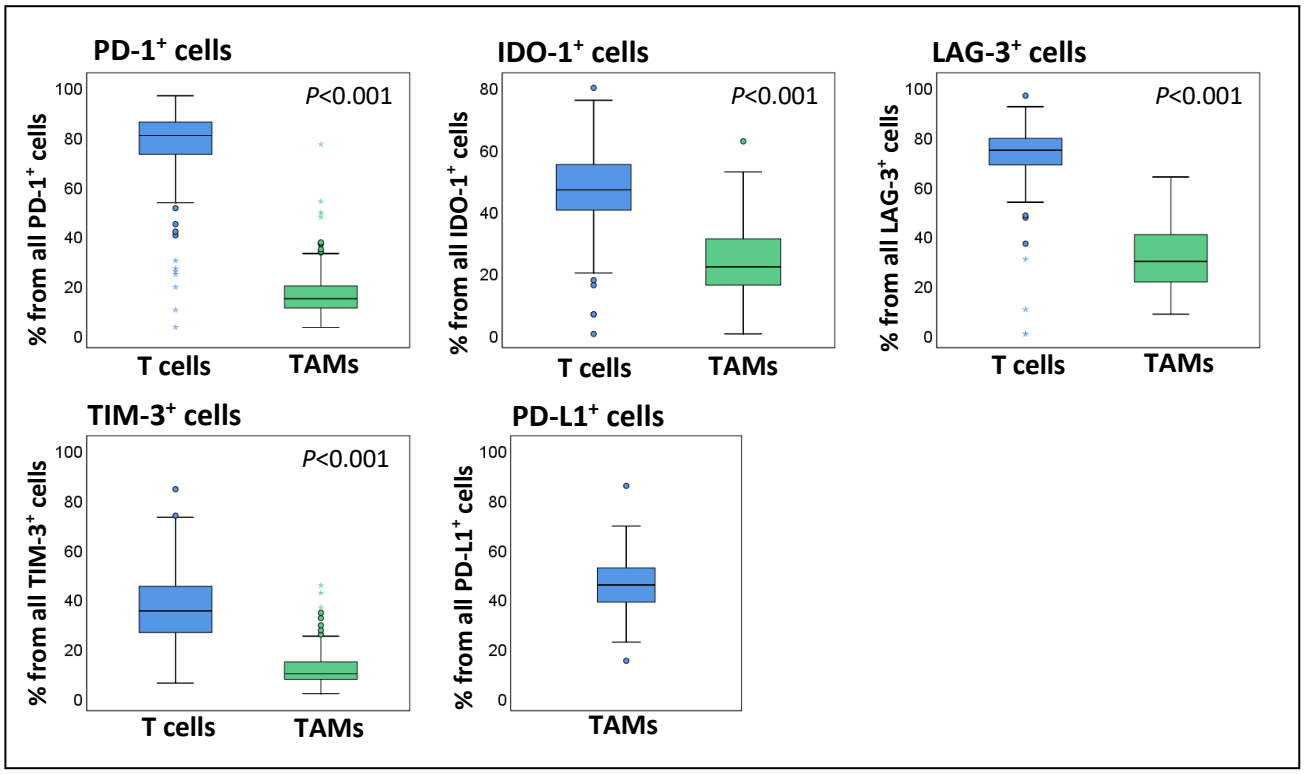

Supplementary Figure S7. Checkpoint expression according to the T cell and TAM phenotypes.